International Journal of Science and Engineering Applications
Volume 5 Issue 7, 2016, ISSN-2319-7560 (Online)

Theoretical Study on Mechanism for the Reaction of 2-propargyl radical (C_3H_3) with ammonia (NH_3)

Tien V. Pham
School of Chemical Engineering
Hanoi University of Science and Technology
Hanoi City, Vietnam

Hue M. T. Nguyen
Faculty of Chemistry
Hanoi National University of Education
Hanoi City, Vietnam

Abstract: A theoretical study of the mechanism and kinetics of the reaction of 2-propargyl radical, H_2CCCH, with ammonia, NH_3, has been carried out by ab initio molecular orbital theory based on CCSD(T)/6-311++G(3df,2p)//B3LYP/6-311++(3df,2p) method. The potential energy surface (PES) for the C_3H_3 + NH_3 reaction was established, showing that the reaction has four principal entrance channels. Two H-abstraction reactions from NH_3, leading to propyne or allene + NH_2. The addition reactions start by formation of two intermediates $H_2CCCHNH_3$ and $H_2CC(NH_3)CH$. From these two intermediate states, many other transition states and intermediate states can be accessed, leading to 21 possible products. The reaction has sizable entrance energy barriers, though the H-abstraction entrance channels might contribute significantly at high temperatures, where formation of $HCCCH_3$ + NH_2 is more energetically favorable.

Keywords: *Reaction mechanism, propargyl radical, ammonia, DFT, PES.*

1. INTRODUCTION

Free radicals exhibit high chemical reactivity and diversities. They can react with atoms, molecules or other radicals. Propargyl (C_3H_3) is a free radical reserved much concern over the last two decades. It is known to play an important role in chemistry due to the following reasons: i) it is the first chemical species containing three carbon atoms found in interstellar medium. ii) It is an important intermediate in combustion processes. For example, it occurs with relatively significant concentration in the flames of acetylene, butadiene and benzene as well as in the decompositions of hydrocarbons in mass spectrometry.[1-3] iii) It is also the most important precursor in the formation of single and polycyclic aromatic hydrocarbons (PAHs) as well as of soot particles. For example, the recombination reaction of two propargyl radicals to yield benzene or phenyl radical (C_6H_5) which are viewed as fundamental molecules to form PAHs and soot. As small aromatic radicals such as phenyl, phenylvinyl ($C_6H_5C_2H_2$), naphthyl ($C_{10}H_7$), and their derivatives are believed to play a pivotal role in the formation of naphthalene ($C_{10}H_8$) by HACA (H-abstraction, C_2H_2-addition) reactions and cyclization reactions. The repetition of such a successive abstraction/addition/ cyclization process involving increasingly larger aromatic radicals has been proposed as a possible route to the formation of PAHs which give rise to soot.[2,3] iv) It also takes part in the chemical changing process of oxides of nitrogen (NO_x) and carbon (CO_x) quickly and effectively.[3] The high reactivity of C_3H_3 allows it to react with species which have sustainable closed shell such as H_2O, CO, CO_2, NH_3, and so on.[4,5]

The formation of C_3H_3 has been clarified by many previous theoretical and experimental works.[2-7] There havebeen investigations, both theoretically and experimentally, about the reaction of propargyl radical with other species in the interstellar medium and in combustion systems, including the self-reaction with another propargyl radical, with elements such as H, O(^{3}P), C(^{3}P), or with other hydrocarbon radicals such as CH_3.[8-13] The mechanisms of reactions between propargyl radical with O_2, H_2O, NO, CO, HCNO, OH, H, CH_3, and C_3H_3 were investigated by our group using density functional theory.[5] Reactions of propargyl radical with atoms or with other free radicals usually occur rapidly without energy barriers.[2-4] In contrast, reactions of propargyl with neutral molecules usually have energy barriers.[10,11,19]

There are two reasons why we choose the propargyl radical to study. Firstly, the reactions of propargyl with the oxides of nitrogen NO_x, which are important in processes such as thermal $DeNO_x$ (Process for reducing NO_x emission), NO_x-OUT (Process for reducing NO from fossil-fueled and waste-fueled stationary combustion sources), $RAPRENO_x$ (Rapid reduction of nitrogen oxides) and NO-reburning, are foreshadowed to be barrier-free leading to primary nitroso and nitro derivatives that further undergo a variety of transformations.[8-12] Secondly, the main reaction pathways of propargyl radical with either the hydrogen compounds or the hydrocarbons involves a hydrogen abstraction yielding C_3H_4 whose energy barrier is consistently low.[13-14,19-25] As far as we are aware, little is actually known about the reactions of C_3H_3 with other simple molecules such as ammonia and hydrogen halides. In view of such scarcity of quantitative information, and in relation to our continuing study on the chemistry of propargyl radical, we set out to investigate the reaction of C_3H_3 with ammonia (NH_3). Because we know that gasification of solid fuels such as coal, biomass and peat results in a fuel gas containing high concentrations of NH_3. This ammonia may give rise to high NO_x emissions when the fuel gas is burned. In addition, ammonia is also known to be released from the processes using urea in agriculture. More recently, various workers have measured the ammonia lost from urea applied to the surface of soils. Ernst and Massey (1960) shown that initial soil moisture increased process of losing NH_3 from surfaced-applied urea. The ammonia will likely escape to the atmosphere according to the following reaction:

$$(NH_2)_2CO + H_2O + \text{urease} \rightarrow NH_3 + H_2NCOOH \rightarrow 2NH_3(gas) + CO_2(gas)$$

where, Urease is a naturally occurring enzyme that catalyzes the hydrolysis of urea to unstable carbamic acid. Rapid decomposition of carbamic acid occurs without enzyme catalysis to form ammonia and carbon dioxide.[26,27] Moreover, the environment with pH around 9.0 may cause soils around the applied urea particle to increase ammonia volatilization. The amount of ammonia volatilization depends on several environmental factors, including temperature, pH, and the soil water content. [28-31]

In this study, we have theoretically mapped out the potential energy surface (PES) describing the C_3H_3 + NH_3 reacting system, in order to obtain essential information on the reaction rates and products distribution.

2. COMPUTATIONAL METHODS

We have characterized the mechanism of the reaction between C_3H_3 and NH_3 by quantum-chemical calculations based on the density functional theory (DFT) with the popular hybrid B3LYP functionals in conjunction with the dp-polarized plus diffuse functions 6-311++G(3df,2p) basis set.[15-18] Vibrational frequencies and zero-point vibrational energies (ZPVE) corrections are obtained at the same level of theory. The stationary points were identified for local minima or transition states according to their vibrational analysis in which the reactants, intermediates, and products possessed all real frequencies, whereas a transition state and only one imaginary frequency. Transition states were then verified by IRC for the connectivity of the reactants and products.

In order to further improve the relative energies for all the species, single-point energy calculations were then computed using the coupled-cluster level of molecular orbital theory, incorporating all the single and double excitations plus perturbative corrections for the triple excitations, CCSD(T)/6-311++G(3df,2p), corrected for ZPE. Geometries of all species in this system have been optimized by means of the Gaussian 09 software package.[19] The predicted full PES of the C_3H_3 + NH_3 system is presented in figure 1S of the Supporting Information (SI)[32] and the energetically low-lying reaction paths are shown in figure 4.

3. RESULTS AND DISCUSSION

3.1 Reactivity prediction

In order to determine the dominant channels in the reaction system of C_3H_3 with NH_3, we calculated and analyzed the energies of critical molecular orbitals (MO) which are shown in table 1.

Table 1. Energy values of HOMO and LUMO at the CCSD(T)/6-311++G(3df,2p) level

	E (HOMO) (eV)	E (LUMO) (eV)	ΔE(LUMO-HOMO) (eV)	
C_3H_3	-0.35631 (HOMOα)	0.03930 (LUMOα)	$C_3H_3(\alpha)$ – $NH_3(\alpha)$	0.46734
	-0.39201 (HOMOβ)	0.04206 (LUMOβ)	$C_3H_3(\beta)$ – $NH_3(\alpha)$	0.47010
NH_3	-0.42804 (HOMOα)	0.04349 (LUMOα)	$NH_3(\alpha)$– $C_3H_3(\alpha)$	0.39980
			$NH_3(\alpha)$ – $C_3H_3(\beta)$	0.43550

Application of the frontier molecular orbital (FMO) theory to compute the energy values between the HOMO and LUMO (ΔE). The results in table 1 point out that the minimum energy value (ΔE) corresponds with the LUMO-α energy level of NH_3 and the HOMO-α energy level of C_3H_3. Therefore, when the reaction takes place, electron density will move from C_3H_3 radical to NH_3 molecule to saturate valence state. These results are appropriate to form the sigma bonds in yielding the intermediates such as IS1 and IS5. The images of frontier orbitals are displayed in figure 1.

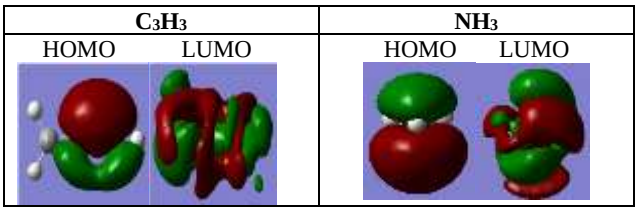

Figure 1. Images of HOMO and LUMO of C_3H_3 and NH_3

3.2 Potential energy surface and reaction mechanism

The optimized geometries of the intermediates, transition states and products at the B3LYP/6-311++G(3df,2p) level are shown in figure 2a and figure 2b. The detailed potential energy surface obtained at the UCCSD(T)/6-311++G(3df,2p)//B3LYP/6-311++G(3df,2p) level is presented in figure 1S (see the Supporting Information), and the important reaction channels of the potential energy surface are simplified and shown in figure 3.

The scheme of the C_3H_3 + NH_3 reaction is presented in figure 2S of the SI. Theoretical prediction of relative energies ΔE (kcal/mol) for reactants, intermediates, transition states, and products of the reaction in different levels of theory are listed in table 2. Table 3 shows a comparison of calculated heats of reaction for the C_3H_3 + NH_3 system with available experimental data. In the SI, table 1S shows Gibbs free energies (ΔG) and entropies (ΔS) for different conditions, table 2S lists harmonic vibrational frequencies of the species considered, table 3S contains their cartesian coordinates and table 4S mentions theoretical predication of single point energy and ZPVE for reactants, intermediates, transition states, and products of the C_3H_3 + NH_3 reaction in two different levels. To help us understand the low-energy reaction pathways for the C_3H_3 + NH_3 system, we only concentrate on analyzing the main reaction channels illustrated in figure 3.

Table 2. Relative energies (kcal/mol) of all the stationary points considered.

Structures	B3LYP/ 6-311++G(3df,2p)	CCSD(T)/ 6-311++G(3df,2p)	Structures	B3LYP/ 6-311++G(3df,2p)	CCSD(T)/ 6-311++G(3df,2p)
$C_3H_3 + NH_3$ (1)	0.0	0.0	T8/P3	22.15	21.84
$H_2CCCHNH_2 + H$ (P1)	32.51	27.31	T8/12	23.65	20.93
$HCCCH_3 + NH_2$ (P2)	17.09	14.21	T4/3	34.58	34.34
$H_2CCCH_2 + NH_2$ (P3)	15.67	15.05	T0/P3	21.96	26.14
$H_2CCCHNH + H_2$ (P4)	12.03	12.75	T6/7	90.00	85.57
$H_2CCHCNH_2+H$ (P5)	49.80	42.62	T9/P6	22.84	18.71
$H_2CCHCHNH + H$ (P6)	18.11	9.75	T1/4	42.51	41.99
H_3CCCNH_2+H (P7)	33.63	26.87	T1/3	39.09	37.08
$CH_3NH_2+C_2H$ (P8)	62.97	56.13	T4/P6	18.39	12.98
H_2CCCH_3+NH (P9)	122.43	113.07	T3/P1	33.34	31.40
$H_2CNH_2 + C_2H_2$ (P10)	18.94	16.72	T17/P15	11.99	11.5
$H_2CCNH + CH_3$ (P11)	4.25	4.83	T3/P4	54.94	56.91
$HCCNH + CH_4$ (P12)	0.08	2.18	T3/P7	34.96	32.00
$H_3CCN + CH_3$ (P13)	-17.8	-22.97	T1/6	94.11	93.35
$C_2H_4 + CNH_2$ (P14)	27.22	25.34	T7/P5	59.25	59.16
$C_2H_4 + HCNH$ (P15)	4.98	3.38	T5/8	42.73	40.06
$C_2H_5 + HCN$ (P16)	-9.8	-15.35	T4/9	21.59	19.54
$C_2H_5 + CNH$ (P17)	3.08	-1.67	T3/P2	23.36	21.63
$C_2H_2+HCNH_3$ (P18)	86.21	82.24	T12/P12	87.57	87.64
$H_3CCH_2CN + H$ (P19)	-0.13	-11.81	T4/10	34.05	34.51
cyc-$HCCHNHCH_2+H$ (P20)	42.14	31.19	T10/11	49.79	45.94
$HCCCH_2NH_2+H$ (P21)	40.12	30.27	T11/20	54.02	51.56
I1	34.69	35.51	T11/P10	28.97	28.09
I3	-3.5	-6.46	T10/P3	21.31	22.31
I4	-30.72	-31.66	T12/13	13.05	8.52
I5	40.33	37.36	T13/P13	-5.3	-10.22
I6	54.4	51.87	T4/14	36.55	35.14
I7	34.18	30.64	T16/17	14.43	12.41
I8	-27.51	-30.46	T14/P5	55.41	52.37
I9	-6.28	-11.33	T14/P14	35.49	33.53
I10	2.6	-1.73	T3/15	38.65	37.38
I11	5.39	-0.16	T3/16	31.72	30.62
I12	-27.42	-31.70	T6/P18	89.38	86.3
I13	-30.16	-35.95	T15/18	48.48	45.85
I14	20.06	15.30	T1/20	103.18	98.28
I15	-7.76	-10.89	T16/18	24	23.05
I16	-28.73	-31.45	T11/21	45.31	41.11
I17	-12.99	-18.74	T20/P21	45.43	42.25
I18	-15.36	-19.57	T18/P19	4.64	-0.70
I19	-24.88	-30.72	T17/18	24.3	21.42
I20	41.77	38.19	T21/P20	46.59	42.04
I21	43.03	37.72	T15/16	33.6	31.31
T0/5	40.29	39.62	T16/19	18.93	14.17
T0/P2	23.29	23.94	T16/18	22.09	21.15
T0/1	34.15	36.62	T19/P19	4.7	-2.24
T1/P1	39.39	41.29	T19/P16	-1.76	-6.64

(a) The addition pathways. It can be seen from figure 3, there are two addition entrance channels of the reactants. Addition of NH_3 onto C_3H_3 is possible at two carbon atoms. The attack at the central carbon, giving rise to an intermediate I_5($H_2C=C(NH_3)$-CH) through TS_1, occurs without a pre-association complex and with a high energy barrier of 39.6 kcal/mol. This process is predicted to be endothermic by 37.36 kcal/mol with a tight transition state. The C-N distance in TS_1 (see in figure 2b) is quite long (1.8 Å), which is suitable with structure of a transition state. From the intermediate I_5, an isomeric intermediate I_8 ($H_2C=C(NH_2)$-CH_2) was formed via a H-migration transition state TS_{21} with the energy barrier of 2.7 kcal/mol. Conformer I_8 lies below the reactants by 30.46 kcal/mol. Once I_8 is formed, it can be converted in two ways, namely (i) a NH_2-loss giving allene ($H_2C=C=CH_2$) P_3 by crossing through the transition state TS_5 (shown in figure 2b) with an 21.84 kcal/mol barrier above the reactants, and (ii) a 1,7-H-shift yielding I_{12} (H_3C-C(NH)=CH_2, -31.7 kcal/mol) via TS_6 overcoming an energy barrier of 51.39 kcal/mol. The lower TS of the two, TS_6, still lies 20.93 kcal/mol above the energy of the free reactants. The formation of the product P_3 ($H_2C=C=CH_2 + NH_2$) from the channel

passing through three transition states (TS_1, TS_{21}, TS_5) and two intermediate states (I_5, I_8) is endothermic by 15.05 kcal/mol. Following the formation of I_{12}, there are two reaction channels, of which one goes directly to products P_{11} ($H_2CCNH + CH_3$) without an exit energy barrier, while the other takes place via transition state TS_{31} at 8.52 kcal/mol above the reactants, forming intermediate I13 (H_3C-C(N)-CH_3, which is by far the lowest-energy isomer of the PES at -35.95 kcal/mol. I13, however, is relatively unstable with respect to a C-C bond cleavage via TS_{32} (-10.22 kcal/mol) producing P_{13} ($H_3CCN + CH_3$, -22.97 kcal/mol), the lowest-lying fragment products.

The data in figure 3 shows that the energy of product P_{13} (-22,97 kcal/mol) is lower than that of the product P_{11} (4.83 kcal/mol) by 27.8 kcal/mol, but the pathway producing P_{13} has to pass through many high energy barriers. Thus, the product P_{11} is more easily formed while P_{13} is the most stable one compared to all others of the PES.

Table 3. Comparison of Calculated Heats of Reaction for $C_3H_3 + NH_3$ with Experimental Data.

Species	B3LYP/6-311++G(3df,2p) (kcal/mol)[a]	CCSD(T)/6-311++G(3df,2p) (kcal/mol)[a]	Experiment (*) (kcal/mol)
$H_2CCCHNH_2$+H (P1)	32.15	26.95	---
$HCCCH_3$+NH_2 (P2)	17.82	14.12	14.01±1
H_2CCCH_2+NH_2(P3)	15.49	14.87	15.74±1
$H_2CCCHNH$+H_2(P4)	12.36	12.81	---
$H_2CCHCNH_2$+H (P5)	49.30	42.12	---
$H_2CCHCHNH$+H (P6)	17.48	9.12	---
H_3CCCNH_2+H (P7)	33.24	26.48	---
H_2CNH_2+C_2H_2(P10)	18.56	16.34	16.93±0.2
$H_2CCNH + CH_3$(P11)	4.09	4.67	---
$HCCNH + CH_4$(P12)	0.04	2.14	---
$H_3CCN + CH_3$(P13)	-17.96	-23.13	-21.49±2
$C_2H_4 + CNH_2$(P14)	26.67	24.79	---
C_2H_4 + HCNH (P15)	4.42	2.82	---
C_2H_5 + HCN (P16)	-10.04	-15.59	-14.91±0.7
C_2H_5+CNH (P17)	3.16	-1.59	-0.06±1.5
H_3CCH_2CN + H (P19)	-0.63	-12.30	-9.48±2
cyclo-$HCCHNHCH_2$+H (P20)	41.04	30.09	---
$HCCCH_2NH_2$ + H (P21)	39.76	29.92	---

[a] The exothermicity for the formation of $C_3H_3 + NH_3$ was calculated on the basic of the experimental heats of formation at 0 K, (*) from reference.[19]

Attackon the terminal carbon of C_3H_3, is initiated by formation of a pre-reactive complex, followed by a high energy barrier TS3 of 36.62 kcal/mol, yielding I_1 ($H_2C=C=CH-NH_3$, 35.51 kcal/mol). The distance of 1.63 Å for the C-N bonding TS_3 (see in Fig. 2b) is now much shorter than that in TS_1 above. In both cases of the initial addition reaction paths, the attack angle is around 105-118º and the ammonia moiety apparently exhibits a similar configuration. As shown in figure 3, the I_1 intermediate can first isomerize to I_3 (H_3C-C=CH-NH_2, - 6.46 kcal/mol) via TS_{13} with a small 1.57 kcal/mol barrier; followed either by isomerization to the open-chain I_{16} (H_3C-CH=CH-NH, - 31.45 kcal/mol) via the 1,4-H-shift TS_{38} with a rather high 37.08 kcal/mol barrier, or by fragmention to product P_2 ($HCCCH_3 + NH_2$) by breaking the C-N bond via TS_{23} with a barrier of 28.09 kcal/mol. The overall exothermicity of the process leading to the product P_2 is -14.21 kcal/mol. From intermediate I_{16}, there are three other isomerization channels, leading to intermediates I_{17} (H_2C-CH_2-CH=NH), I_{18} (H_3C-CH_2-C=NH), and I_{19} (H_3C-CH_2-CH=N) with isomerization barriers of 43.86, 52.6, and 45.62kcal/mol, respectively. A 1,4-H shift connects I_{17} and I_{18} with the energy barrier via TS_{47} of 40.16 kcal/mol, where the angle N-C-C changes slightly from 123° in I_{17} to 137° in I_{18}. I_{17} fragmentation over the 30.24 kcal/mol barrier height of TS_{16} produces product P_{15} (C_2H_4 + HCNH) with 3.38 kcal/mol of endothermicity. In figure 3, one sees that product P_{19} (H_3C-CH_2-CN + H) can be formed in two ways; one taking place via the intermediate I_{18}, while the other via the intermediate I_{19}. The energy of the transition state TS_{54} in the first path is lower than that of TS_{46} in the latter by only 1.54 kcal/mol. Furthermore, two products, namely P_{16} (C_2H_5 + HCN) and P_{17} (C_2H_5 + CNH), can also form from I_{19} and I_{18}, respectively. P_{17} was produced directly from I_{18} without any exit energy barrier, whereas the product P_{16} was produced by the C-C bond-breaking process with anenergy barrier of 6.46 kcal/molbelow the entrance point. It is clear that product P_{16} is more stable than product P_{17}. Formation of both of these is exothermic with relative energies of -15.35 kcal/mol and -1.67 kcal/mol, respectively. The I_1 intermediate formed in the current addition reaction can also undergo isomerization to another isomer I_4 (H_2C=CH-CH-NH_2, -31.66 kcal/mol,) via TS_{12} with a 6.48 kcal/mol barrier. This barrier is higher than that of the earlier process forming the isomer I_3 with only 1.57 kcal/mol barrier height. This thelatter path is therefore expected to contribute less significantly. The I_4 intermediate further dissociates to product P_6 ($H_2CCHCHNH$ + H) via TS_{14} with a 12.98 kcal/mol barrier above the reactants. I_4 can also isomerizes to I_9 (H_2C=CH-CH_2-NH, -11.33 kcal/mol) by a 1,7-H shift via TS_{22} with 19.54 kcal/mol above the entry point, and then breaking the C-H bond in I_9 forming the same product P_6 via TS_{11} costing 30.04kcal/mol energy. The isomerization transition state (TS_7) between I_4 and I_3 is also

located; its energy is 34.34 kcal/mol higher than that of the reactants.

We can see that both of the addition pathways illustrated in figure 3 can produce many different products. The entrance transition structure, TS_1 (39.62 kcal/mol), is found to be higher in energy than TS_3 (36.62 kcal/mol); accordingly, it is concluded that the latter pathway takes place relatively faster than the former. As both these transition states are high in energy, all products formation through these two channels is controlled mainly by TS_1 and TS_3, and is expected to be kinetically unfavorable.

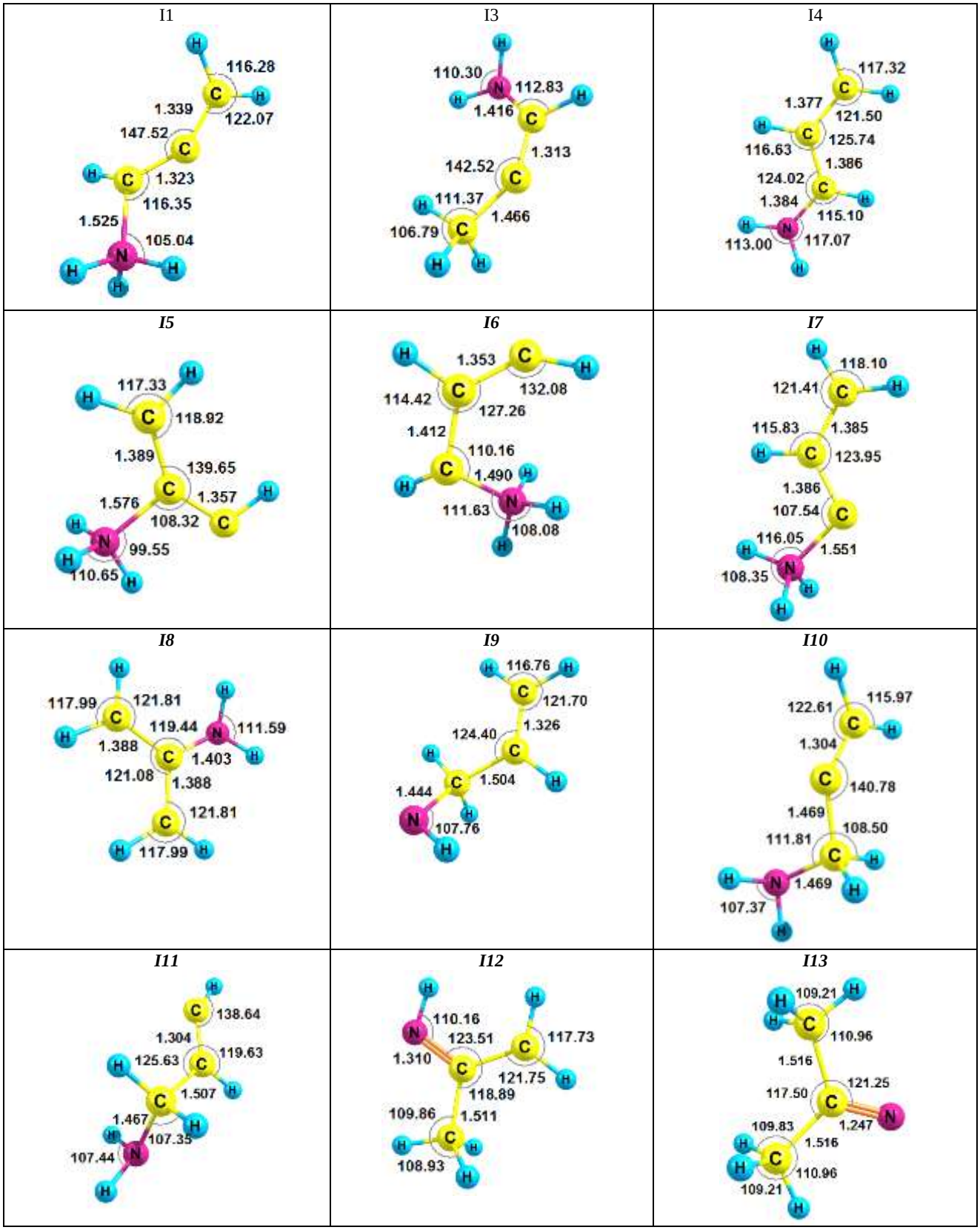

I14 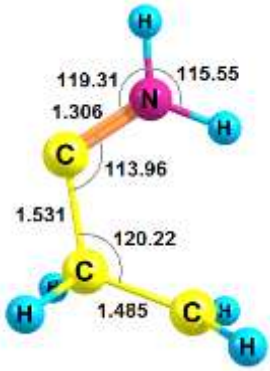	***I15*** 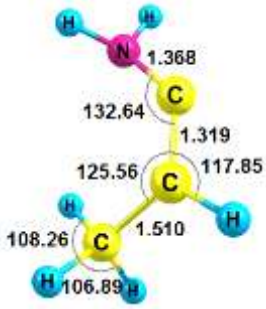	***I16*** 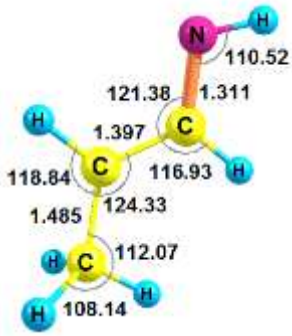
I17 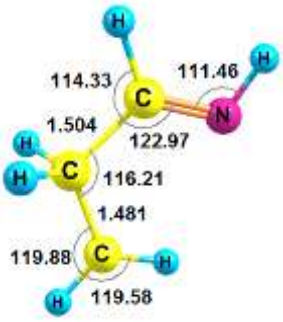	***I18*** 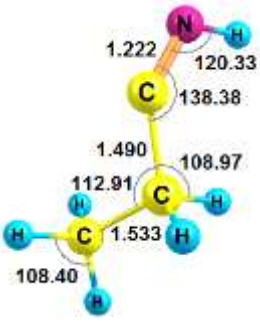	***I19*** 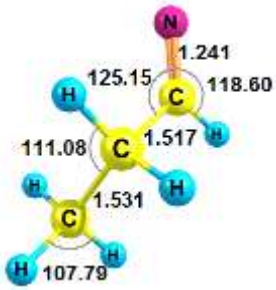
I20 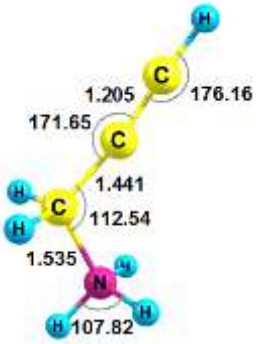	***I21*** 	***P1*** 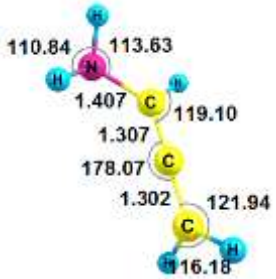
P2 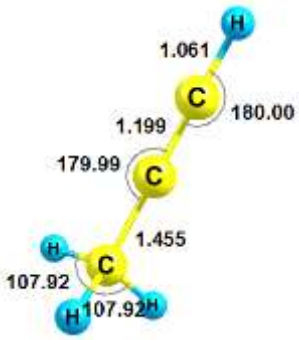	***P3*** 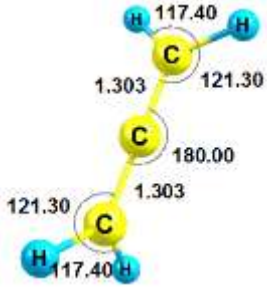	***P4*** 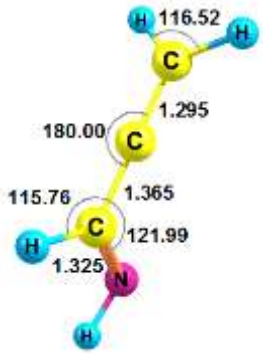
P5	***P6***	***P7***

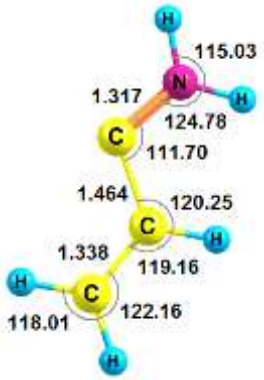	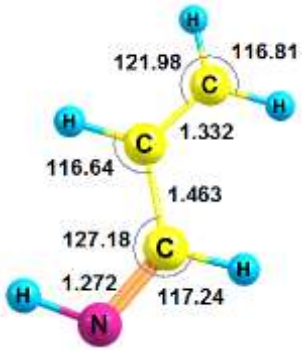	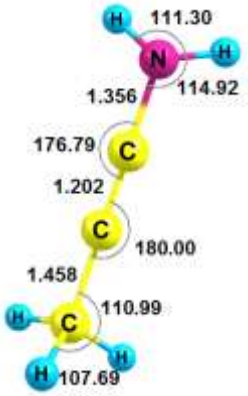
P8 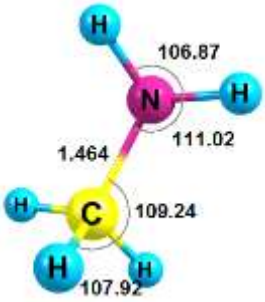	***P8*** 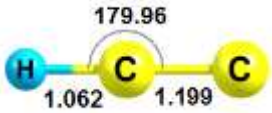	***P9*** 
P9 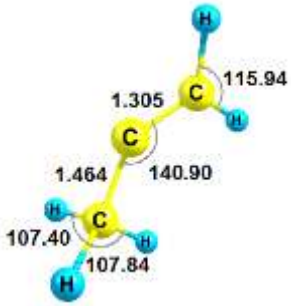	***P10*** 	***P10*** 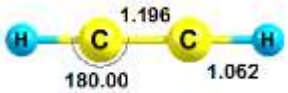
P11 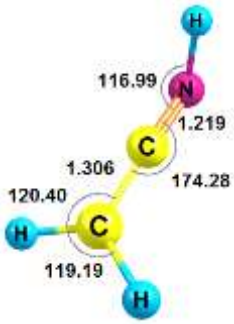	***P12*** 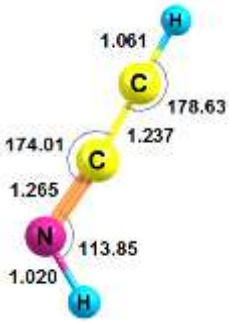	***P13*** 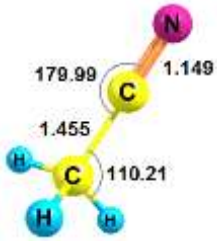
P14 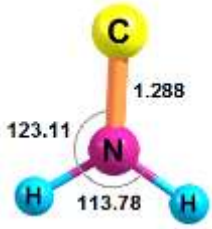	***P14*** 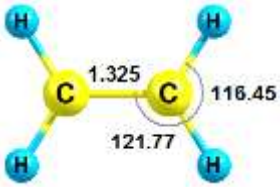	***P15*** 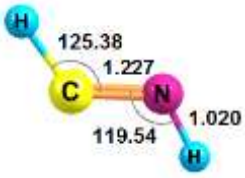
P16	***P17***	***P18***

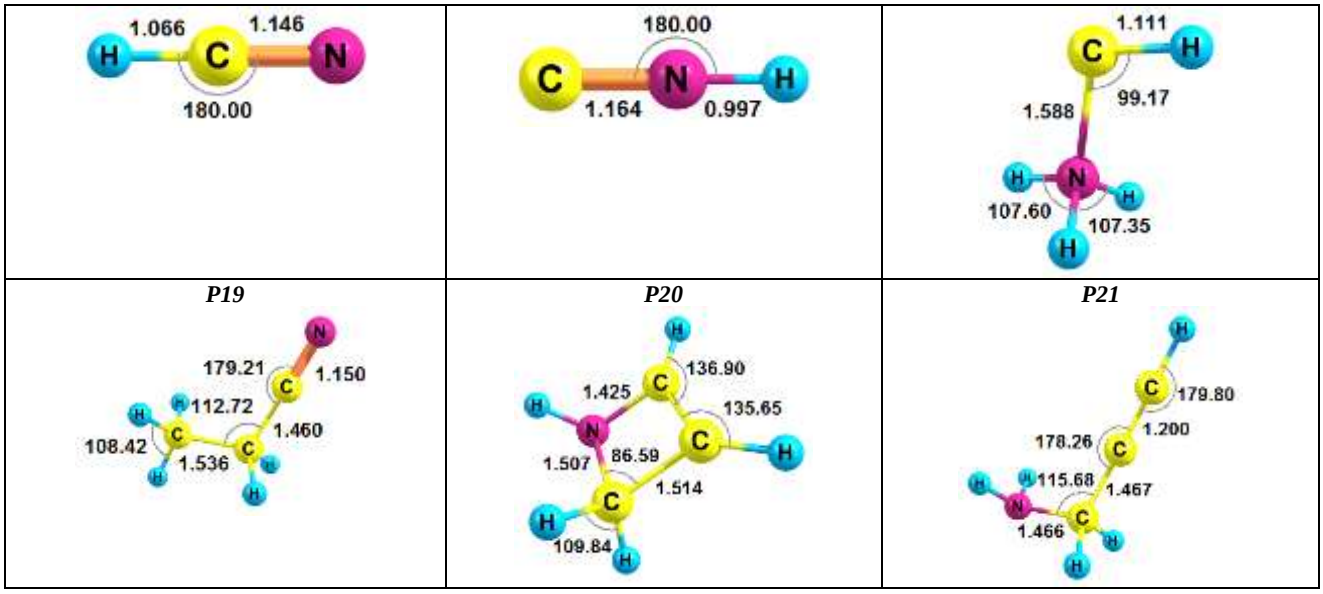

Figure 2a. Optimized geometries of the intermediate states and products involved in the reaction of C_3H_3 + NH_3 at the B3LYP/6-311++G(3df,2p) level. (The bond lengths are given in angstroms and angles in degrees).

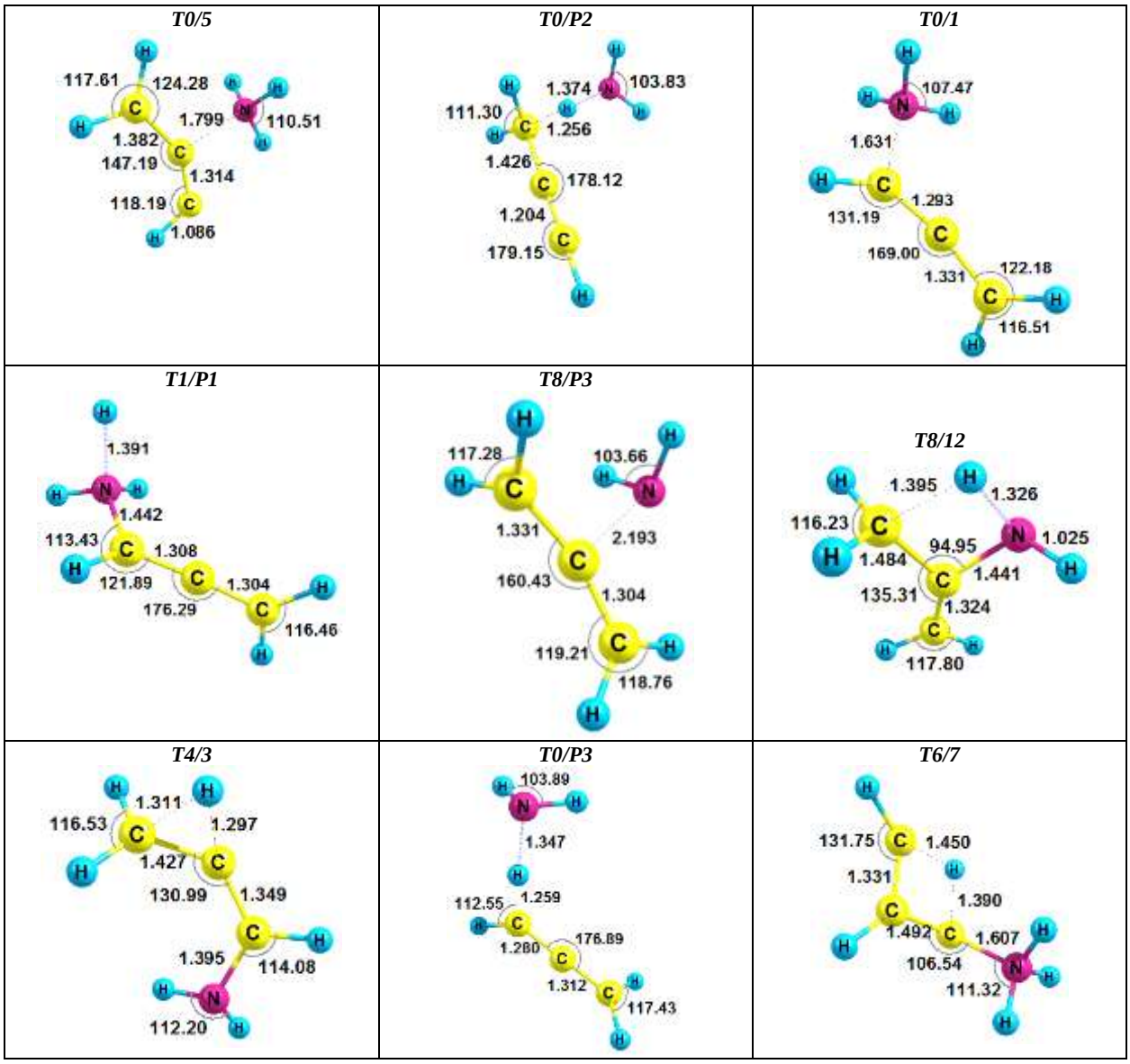

T9/P6 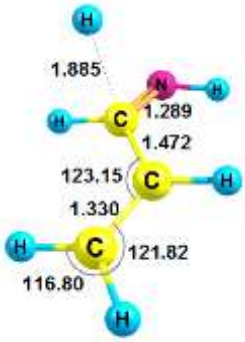	***T14*** 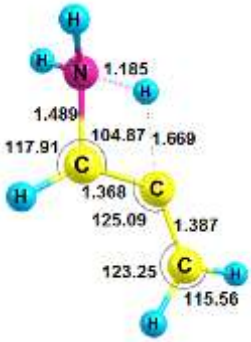	***T1/3*** 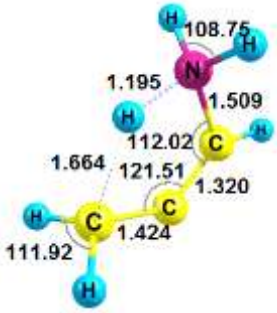
T4/P6 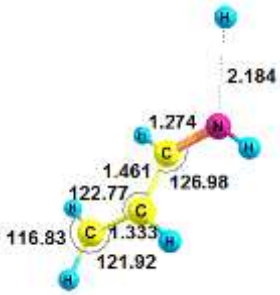	***T3/P1*** 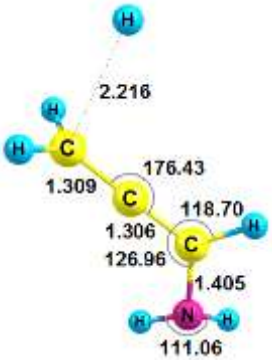	***T17/P15*** 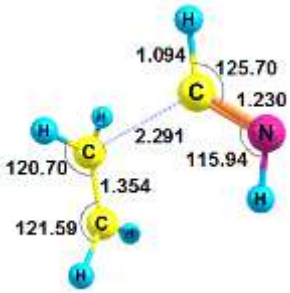
T3/P4 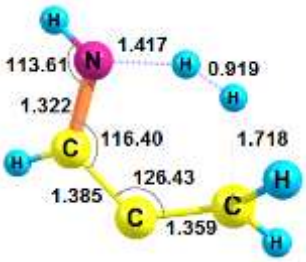	***T3/P7*** 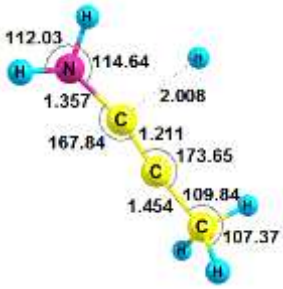	***T1/6*** 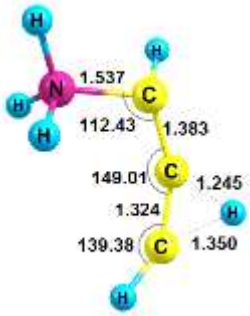
T7/P5 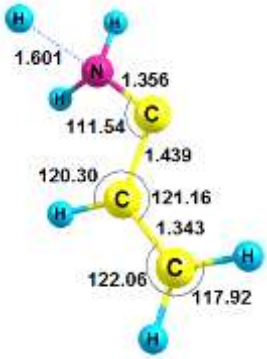	***T5/8*** 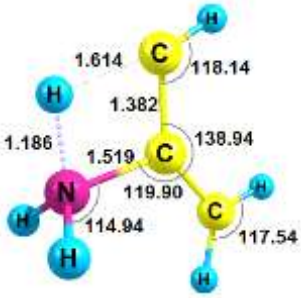	***T4/9*** 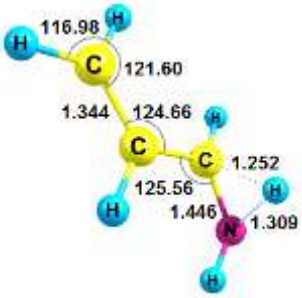
T3/P2 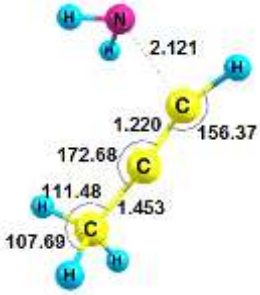	***T12/P12*** 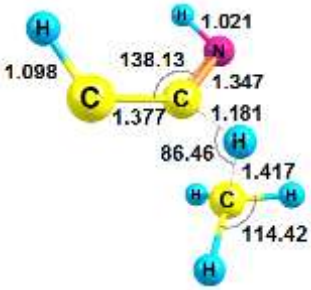	***T4/10*** 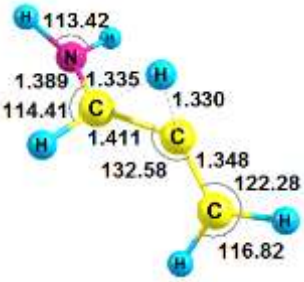

T10/11 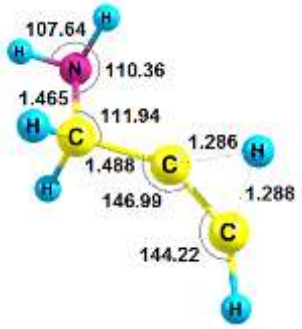	***T11/20*** 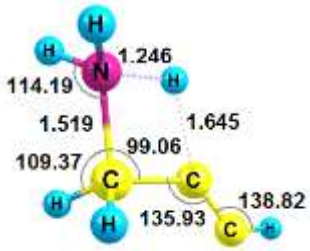	***T11/P10*** 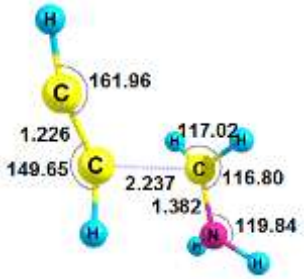
T10/P3 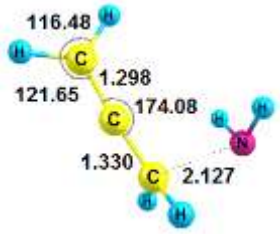	***T12/13*** 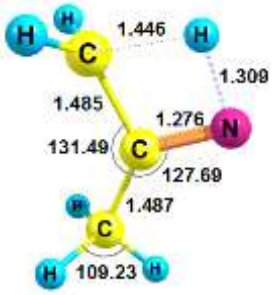	***T13/P13*** 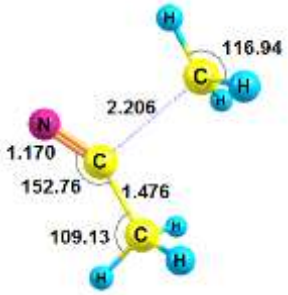
T4/14 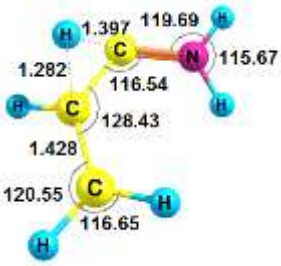	***T16/17*** 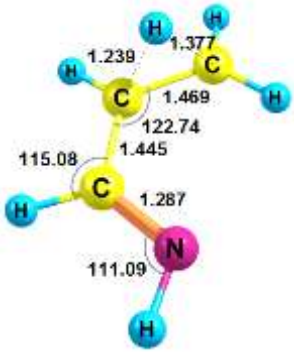	***T14/P5*** 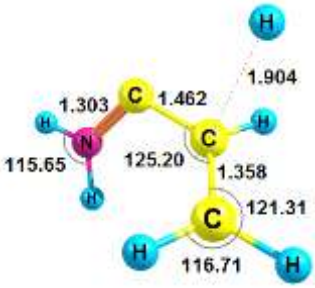
T14/P14 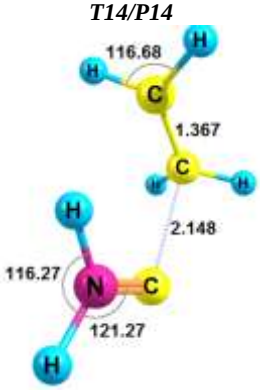	***T3/15*** 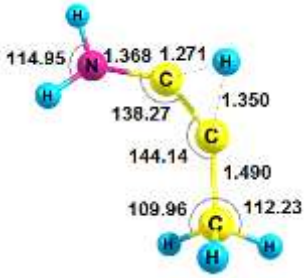	***T3/16*** 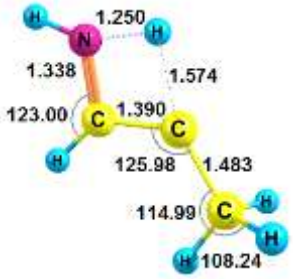
T6/P18 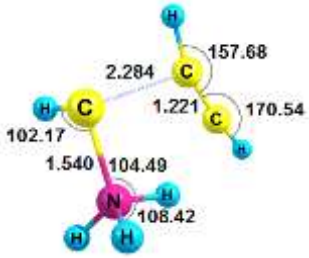	***T15/18*** 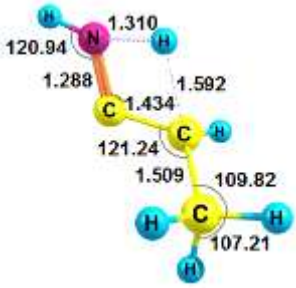	***T1/20*** 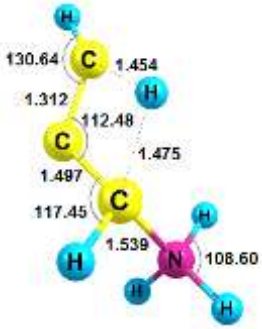

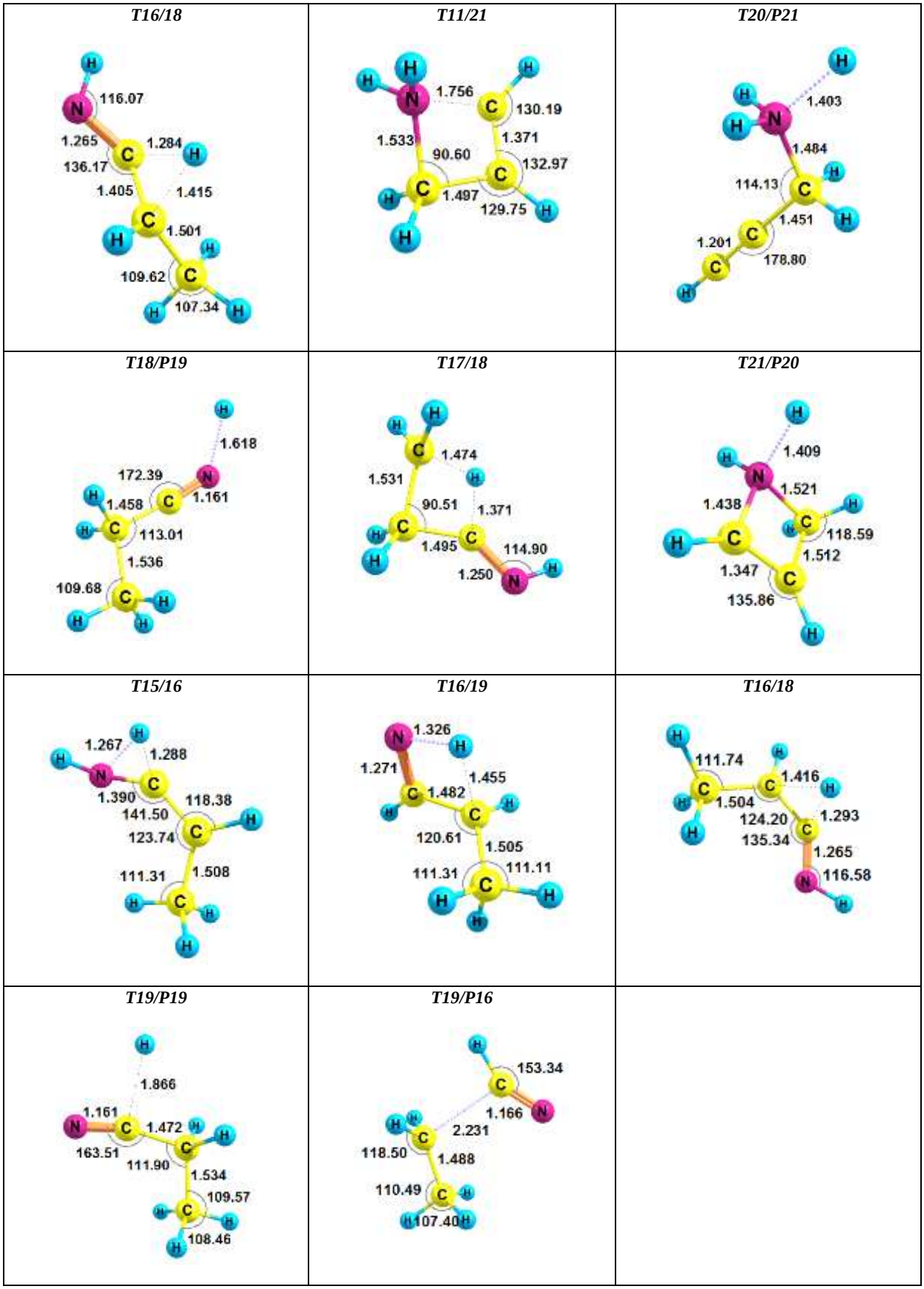

Figure 2b. Optimized geometries of the transition states involved in the reaction of C_3H_3 + NH_3 at the B3LYP/6-311++G(3df,2p) level. (The bond lengths are given in angstroms and angles in degrees).

(b) The hydrogen abstraction pathway. The figure 4 shows that H-abstraction takes place in two channels. The first abstraction channel creates P_2 via only one transition state TS_2 with an energy barrier of 23.94 kcal/mol. Although not having a pre-reactive complex at the beginning of this pathway, the products are formed in a complex with a relative energy value of 12.39 kcal/mol above the energy of the free reactants, before separating without an exit barrier. In the structure of TS_2 (see in figure 2b), when the molecular ammonia approaches the propargyl radical, one of three hydrogen atoms abstracts from ammonia at the distance of 1.374 Å to bond with the carbon atomat the distance of 1.256 Å. In this case, the bond lengths of N…H and C…H are longer than the experimental bond lengths of them[33] about 0.355 and 0.166 Å, respectively. The latter is slightly stable with respect to the separated fragments P_2 ($HCCCH_3 + NH_2$, 14.21 kcal/mol). The distance between H and N in the Com1 is elongated by 1.459Å when going from the TS_2 to Com1. The complex further dissociates to P_2 without transition state. Moreover, it is easy to realize that, the product P_2 is also produced by the additional reaction mechanism as discussed above. Comparing these two mechanisms, one finds that, relatively, the latter mechanism takes place more readily than the former mechanism.

Product P_3 is formed by the second abstraction channel through transition structure TS_8 (shown in Figure 2b) with an energy barrier of 26.14 kcal/mol. In the geometry of TS_8, the distances of N…H and C…H are calculated to be about 1.347 and 1.259Å, respectively; the angle C-C-H changes by more than 61º from 180º in C_3H_3 to 128.42º in TS_8, which suggests that this transtion is a critical motion in this transition state, and relates to the re-hybridisation of the carbon atom from sp to sp^2. Dissociation to the separated products $H_2CCCH_2 + NH_2$ (P_3) occurs by anextremely small dissociation energy of 0.7kcal/mol compared to the complex ($H_2C{=}C{=}CH_2\ldots NH_2$, 14.35 kcal/mol). In this process there is no exit barrier for the loose bond cleavage. In the final product, the newly formed C-H bond length is shortened to 1.08 Å in H_2CCCH_2. Formation of product, $H_2CCCH_2 + NH_2$, is found to be endothermic by 15.05 kcal/mol at the CCSD(T)/6-311++G(3df,2p)//B3LYP/6-311++G(3df,2p) level.

It is obvious that formation of product P_2 via TS_2 is more favorable than product P_3 formed through TS_8.

The results given above clearly demonstrate that the hydrogen abstraction is preferred over the additional reaction.

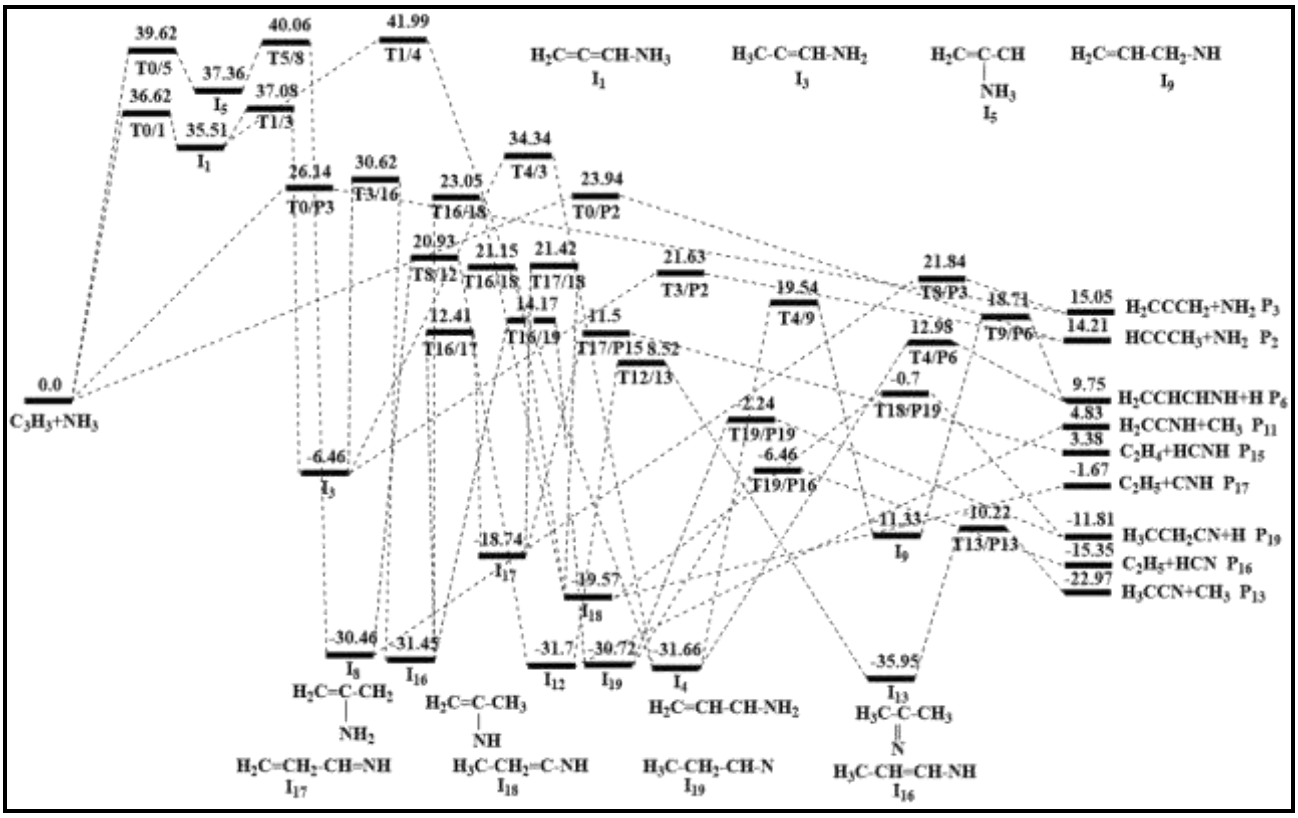

Figure 3. The simplified potential energy surface of the $C_3H_3 + NH_3$ reaction. Energies are in units of kcal/mol calculated at the CCSD(T)/6-311++G(3df,2p)//B3LYP/6-311++G(3df,2p) + ZPVE level.

4. CONCLUSION

By application of the density functional theory, we have optimized geometric structures of reactants, intermediate substances, transition states, and products of the $C_3H_3 + NH_3$ reaction system, based on the CCSD(T)/6-311++G(3df,2p)//B3LYP/6-311++G(3df,2p) methods.

In the present theoretical study, we have mapped in detail the $[C_3H_6N]$ potential energy surface, with emphasis on the sections guiding the four main reaction routes for the $C_3H_3 + NH_3$ reaction, namely the hydrogen abstractions and addition reactions. Calculated results indicate that products of this reaction can be P_1 to P_{21} as shown in the full PES. The formation of P_2 ($HCCCH_3 + NH_2$) is the most energetically favorable. However, the product $H_3CCN + CH_3$ (P_{13}) is the most stable product in energy. Calculated enthalpies of

formation for five reaction pathways P_2, P_3, P_{10}, P_{13}, P_{16}, P_{17}, and P_{19} are in good agreement with experimental data, which suggests that the theoretical methodology is reliable.

We find that the hydrogen abstraction is expected to dominate at all temperatures. However, due to its rather lower-lying energies of products, the addition emerges as a novel channel that could contribute significantly at higher temperatures.

In terms of thermodynamics, all products of this reaction are possible to present at the investigated condition. This study is a contribution to the understanding of the reaction mechanisms of the propargyl radical with many small radicals and molecules in the atmosphere and combustion chemistry.

5. ACKNOWLEDGMENTS

We thank the National Foundation for Science and Technology Development (Nafosted), Vietnam, which has sponsored this work.

6. REFERENCES

[1] J. A. Miller, M. J. Pilling, and J. Troe, *Proc. Combust. Inst.* **2005**, *30*, 43-88.

[2] Wei QuanTian, Yan Alexander Wang;*J. Org. Chem*. **2004**, *Vol.69 (13)*, 4299-4308.

[3] Ikchoon Lee, Chan Kyung Kim, Bon-Su Leea,Tae-Kyu Ha; *J. Mol. Struct. (Theochem)*.**1993**, *279*, 191-205.

[4] S. R. Schofield,N. J. Curson, M. Y. Simmons, O. Warschkow, N. A. Marks, H. F. Wilson, D. R. McKenzie, P. V. Smith, M. W. Radny; *e-J. Surf.Sci. Nanotech*.**2006**, *Vol. 4*, 609-613.

[5] HemaMunjal, K L Baluja; *J. Phys. B: At.Mol. Opt. Phys*.**2007**, *40*, 1713.

[6] Michael D. Hoops and Bruce S. Ault; *The Journal of Physical Chemistry A.* **2008**, *112* (24), 5368-5377.

[7] S. J. Klippenstein, J. A. Miller, and A. W. Jasper, *J. Phys. Chem.A*, **2015**, 119 (28), 7780.

[8] Ya A Dorfman, I M Yukht, L V Levina, G S Polimbetova, T V Petrova, V S Emelyanova; *Russ. Chem. Rev*.**1991**, *60*, 605.

[9] Peter A. Hamilton and Timothy P. Murrells; *J. Chem. Soc., Faraday Trans.* **1985**, *2*, *81*, 1531-1541.

[10] Adam J. Delson, Bruce S. Ault; *The Journal of Physical Chemistry A.* **2006**, *110* (51), 13786-13791.

[11] SlawomirBerski, ZdzisławLatajka; *Chemical Physics Letters*.**2006**, *426*, 273–279.

[12] Hue Minh Thi Nguyen, Shaun Avondale Carl, JozefPeeters, Minh Tho Nguyen; *Phys . Chem. Chem. Phys*. **2004**, *6*, 4111-4117.

[13] Shaun A. Carl, Hue Minh Thi Nguyen, Rehab Ibrahim M. Elsamra, Minh Tho Nguyen, and JozefPeeters; *Journal of Chemical Physics.* **2005**, *122*, 114307.

[14] Frank Jensen; *Introduction to Computational Chemistry*; Second edition; John Wiley & Sons, Ltd. **2007**.

[15] A. D. Becke, Density-functional thermochemistry.III. The role of exact exchange, J. Chem. Phys. 98 (**1993**), 5648.

[16] A. D. Becke, Density-functional thermochemistry.I. The effect of the exchange-only gradient correction, J. Chem. Phys. 96 (**1992**), 2155.

[17] A. D. Becke, Density-functional thermochemistry.II. The effect of the Perdew–Wang generalized-gradient correlation correction, J. Chem. Phys. 97 (**1992**), 9173.

[18] C. Lee, W. Yang, R. G. Parr, Development of the Colic-Salvetti correlation-energy formula into a functional of the electron density, Phys. Rev. B 37 (**1988**), 785-789.

[19] M. J. Frisch, G. W. Trucks, H. B. Schlegel,.., J. A. Pople; *Gaussian, Inc*.,Pittsburgh PA. **2003**.

[20] Matsugi, A.; Suma, K.; Miyoshi, A. Kinetics and Mechanisms of some radicals plus Propargyl Recombination Reactions. *J. Phys. Chem*. A. **2012**, *117*, 7321–7334.

[21] Stephen J. Klippenstein†, James A. Miller*†, and Ahren W. Jasper‡. Kinetics of Propargyl Radical Dissociation.J. Phys. Chem. A. **2015**, 119(28), 7780-7791.

[22] Ruscic, B.; Boggs, J. E.; Burcat, A.; Csaszar, A. G.; Demaison, J.; Janoschek, R.; Martin, J. M. L.; Morton, M. L.; Rossi, M. J.; Stanton, J. F.; Szalay, P. G.; Westmoreland, P. R.; Zabel, F.; Berces, T. *J. Phys. Chem. Ref. Data* **2005**, *34*, 573.

[23] Chase, M. W., Jr. *NIST-JANAF Thermochemical Tables*, 4th ed.; American Chemical Society: Washington, D.C.; American Institute of Physics for the National Institute of Standards and Technology: Woodbury: New York, **1998**.

[24] Hansel, A.; Scheiring, Ch.; Glantschnig, M.; Lindinger, W.; Ferguson, E. E. *J. Chem. Phys.* **1998**, *109*, *1748.*

[25] Maricq, M. M.; Smith, M. A.; Simpson, C. J. S. M.; Ellison, B.B. *J. Chem. Phys*.**1981**, *74*, 6154.

[26] Tisdale, Samuel L.; Nelson, Werner L.; Beaton, James D. (1985), Soil fertility and fertilizers, New York: Macmillan, **1985**, 161–168

[27] Jump up^ Benini, Stefano, Wojciech R. Rypniewski, Keith S. Wilson, Silvia Miletti, Stefano Ciurli, and Stefano Mangani. A new proposal for urease mechanism based on the crystal structures of the native and inhibited enzyme from Bacilus pasteurii: why urea hydrolysis costs two nickels. Structure 7, **1999**, 205-216.

[28] Schwab, G.J. and L.W. Murdock. Nitrogen Transformation Inhibitors and Controlled Release Urea. Extension Report. Lexington, KY: University of Kentucky College of Agriculture, **2005**.

[29] Watson, C.J., et al. "Rate and mode of application of the urease inhibitor N-(n-butyl) thiophosphoric triamide on ammonia volatilization from surface-applied urea." Soil Use and Management, British Society of Soil Science (**2008**): 1-7.

[30] Wells, K.L., L.W. Murdock and H.F. Miller. Urea as a Source of Fertilizer Nitrogen for Crops in Kentucky. Extension Report. Lexington, KY: University of Kentucky College of Agriculture, **1978**.

[31] Jump up^ McInnes, K.J., et al. "Field measurements of Ammonia Loss from Surface Applications of Urea Solution to Bare Soil." Agonomy Journal (**1986**): 192-196.

[32] See supplementary material at http://pubs.acs.org for full PES of C_3H_3 + NH_3, optimized geometries of reactants, intermediates and transition states, vibrational frequencies, and predicted rate coefficients.

[33] O. Bastiansen and B. Beagley, Acta. Chem. Scand. 18, (**1964**), 2077.